

A major purpose of the Technical Information Center is to provide the broadest dissemination possible of information contained in DOE's Research and Development Reports to business, industry, the academic community, and Federal, state and local governments.

Although a small portion of this report is not reproducible, it is being made available to expedite the availability of information on the research discussed herein.



CONF - 8306/21 -- 2

Los Alamos National Laboratory is operated by the University of California for the United States Department of Energy under contract W-7405-ENG-36

LA-UR--83-2411

DE83 017235

TITLE EVOLUTION OF LONG PULSES IN A TAPERED WIGGLER  
FREE-ELECTRON LASER

AUTHOR(S) John C. Goldstein

**NOTICE**  
**PORTIONS OF THIS REPORT ARE ILLEGIBLE.**  
It has been reproduced from the best available copy to permit the broadest possible availability.

SUBMITTED TO The Society of Photo-Optical Instrumentation Engineers  
DARPA Free-Electron Laser Conference  
Eastsound, WA  
June 27-July 1, 1983

**DISCLAIMER**

This report was prepared as an account of work sponsored by an agency of the United States Government. Neither the United States Government nor any agency thereof, nor any of their employees, makes any warranty, express or implied, or assumes any legal liability or responsibility for the accuracy, completeness, or usefulness of any information, apparatus, product, or process disclosed, or represents that its use would not infringe privately owned rights. Reference herein to any specific commercial product, process, or service by trade name, trademark, manufacturer, or otherwise does not necessarily constitute or imply its endorsement, recommendation, or favoring by the United States Government or any agency thereof. The views and opinions of authors expressed herein do not necessarily state or reflect those of the United States Government or any agency thereof.

By acceptance of this article the publisher recognizes that the U.S. Government retains a nonexclusive, royalty-free license to publish or reproduce the published form of this contribution or to allow others to do so, for U.S. Government purposes.

The Los Alamos National Laboratory requests that the publisher identify this article as work performed under the auspices of the U.S. Department of Energy.

**Los Alamos** Los Alamos National Laboratory  
Los Alamos, New Mexico 87545

**MASTER**

## Evolution of long pulses in a tapered wiggler free-electron laser

John C. Goldstein

Los Alamos National Laboratory  
X-1, MS E531, Los Alamos, New Mexico 87545

### Abstract

The evolution of a long pulse (pulse length much greater than the slippage distance) in a tapered wiggler free-electron laser is studied by numerical solution of the 1-D theoretical model for a realistic set of magnet, electron beam, and optical resonator parameter values. Single-pass gain curves are calculated for low and high light intensity. We find that an initial, low-amplitude, incoherent pulse grows into a coherent pulse whose growth rate agrees with the calculated small signal gain. The transient evolution of coherent pulses is calculated for several different cavity length detunings, and a quasi steady-state desynchronization curve is given. The frequency changing behavior of the optical pulse is shown to occur through sideband generation associated with synchrotron oscillations. Pulse evolution with an ideal intracavity high-pass optical filter is calculated.

### Introduction

In this work the evolution of a long optical pulse in a tapered wiggler free-electron laser (FEL) oscillator is studied by numerical solution of the 1-D theoretical model for a realistic set of magnet, electron beam, and optical resonator parameter values. The theoretical model used here is one developed by Colson,<sup>1,2</sup> although other equivalent models<sup>3-5</sup> have been developed. The model is solved first for a series of single-pass gain curves. These curves, which show the amplification of cw coherent light at low and high intensity, are obtained by neglecting all finite pulse effects. They are, nonetheless, reasonable first estimates for the rate of growth of the actual finite optical pulse because, for the physical parameters of the laser system considered here, the slippage distance is much shorter than the pulse length. However, the initial low intensity light in the resonator is not coherent--it is incoherent spontaneous emission. We have studied the development of coherence of such an initially incoherent pulse and find that after 100 to 150 passes through the resonator, the optical pulse has achieved a narrow spectrum, with reasonably smooth electric field amplitude and phase functions, and is growing at a rate predicted by the cw single pass small signal gain curve. Results of this calculation, which should be taken only as an approximate indication of the build-up of light from spontaneous emission, are presented.

The transient evolution of a coherent optical pulse, from low intensity small signal gain conditions to high intensity saturated gain conditions, is then calculated for several different optical resonator lengths and a quasi steady-state desynchronization curve is obtained. A comparison of various optical pulse and electron characteristics at different points along the desynchronization curve is made. The frequency changing behavior ("chirping") of the optical pulse during its evolution is characterized by a discontinuous step noted when strong modulation of the electric field envelope is present with a period about equal to the slippage distance. Finally, the effect of an ideal intracavity optical filter on the evolution of the light is presented.

### Gain curves and the development of coherence

The laser system to be modeled is a linear accelerator driven FEL, with parameter values given in Table 1, in which a pulse of electrons is magnetically guided into the optical resonator where it interacts with a pulse of light while transiting the wiggler magnet. The electron pulse is then dumped out of the resonator while the light pulse reflects from the mirrors and meets a new electron pulse from the linac when it re-enters the wiggler. The axial variation of the wavelength and magnetic field strength of the wiggler are shown in Figure 1. The 1-D mathematical model used to analyze this FEL system is specified in Table 2. Note that we are dealing with a plane polarized wiggler, which accounts for the coupling constant G, but we neglect all higher harmonics of the emitted radiation. A Gaussian mode variation of the on-axis electric field amplitude and phase is taken into account but is not explicitly shown in Table 2.

The cw gain vs optical wavelength for this laser system, ignoring finite pulse effects, is shown in Figure 2. Note that these curves are for an idealized monoenergetic electron beam. The small signal gain is in Figure 2a and the large signal gain is in Figure 2b. Note that the wavelength of peak gain shifts with increasing light intensity: this leads

Table 1: System Parameter Values

<b>Wiggler</b>	
Length	100 cm
Field strength	0.3 T
Wavelength range	2.73-2.42 cm
Energy taper	7.35%
Coupling constant G	0.94
<b>Resonator</b>	
Rayleigh range	62.5 cm
Filling factor	0.78
Design resonant wavelength	10.65 μm
Peak-gain wavelength in resonator	10.35 μm
Round-trip intensity loss	2%
<b>Electron Beam</b>	
Peak current	40 A
Pulse length	0.9 cm
Beam diameter	0.18 cm
Slippage distance	0.038 cm
Initial energy	20.85 MeV

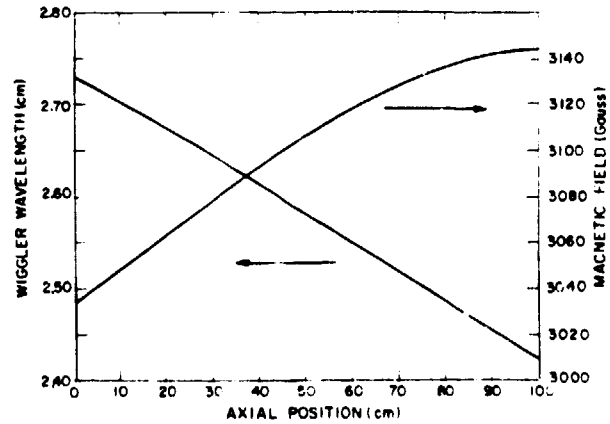


Figure 1. Axial variation of wiggler wavelength and magnetic field amplitude.

Table 2: Equations of Motion

Electrons:

$$\frac{d}{d\tau} \gamma^2 = G(\tau) L_w K_B a_w(\tau) a_B \cos(\xi + \phi) \quad (1)$$

$$\frac{d}{d\tau} \xi = v = 2\pi L_w \left[ \frac{1}{\lambda_w(\tau)} - \frac{1 + 0.5 a_w^2(\tau)}{2\gamma^2 \lambda_B} \right] \quad (2)$$

$$\xi = \int_0^z K_w(z') dz' + K_B z - \omega_B \tau \quad (3)$$

$$\tau = ct/L_w \quad (4)$$

$$G = J_0(y) - J_1(y) \quad (5)$$

$$y(\tau) = \frac{a_w^2(\tau)}{4 + 2a_w^2(\tau)} \quad (6)$$

$$a_w(\tau) = \frac{e B_w(\tau) \lambda_w(\tau)}{2\pi mc^2} ; K_w(\tau) = 2\pi/\lambda_w(\tau) \quad (7)$$

$$a_B = \frac{e E_B \lambda_B}{2\pi mc^2} ; K_B = 2\pi/\lambda_B \quad (8)$$

Light:

$$\frac{\partial}{\partial \tau} E = -2\pi G(\tau) e L_w \rho(u) \left\langle \left\langle \frac{\cos(\xi + \phi)}{\gamma} \right\rangle \right\rangle_{\xi_0} \nu_0 \quad (9)$$

$$E \frac{\partial}{\partial \tau} \phi = 2\pi G(\tau) e L_w \rho(u) \left\langle \left\langle \frac{\sin(\xi + \phi)}{\gamma} \right\rangle \right\rangle_{\xi_0} \nu_0 \quad (10)$$

$$u = z - L_w \tau + B(\tau - 1/2) \quad (11)$$

$$u = (1 - \beta_z) L_w = (\lambda_w/L_w) \lambda_B = N \lambda_B \quad (12)$$

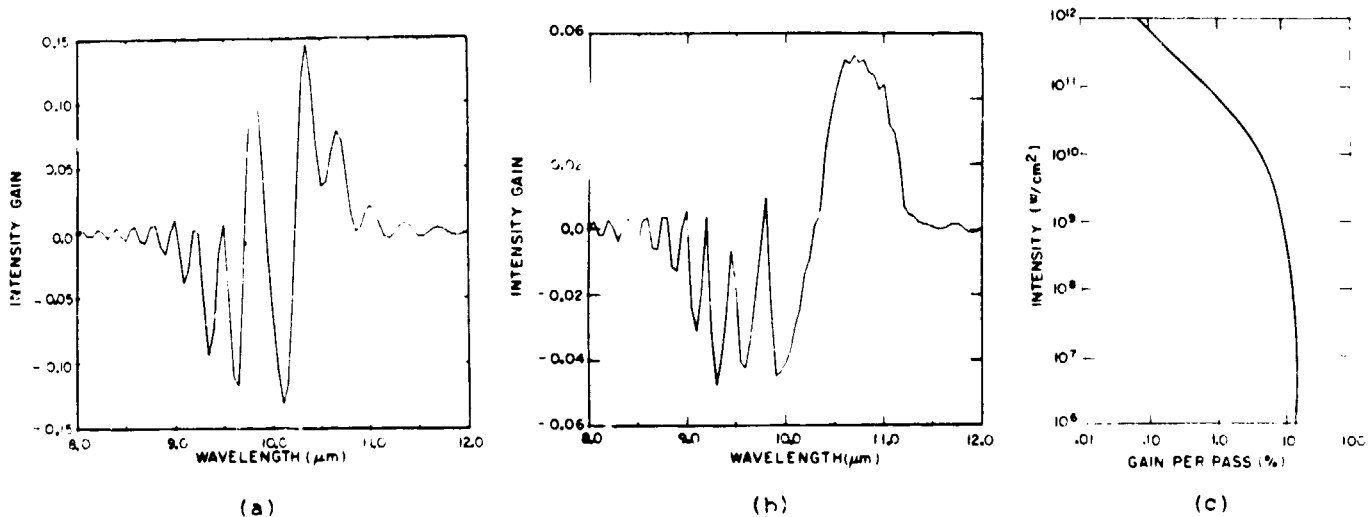


Figure 2. The cw gain curves: (a) small signal; (b) large signal; (c) maximum gain.

to chirping of the optical pulse, which is discussed below. If the maximum gain (at whatever wavelength it occurs) vs intensity is plotted, the curve of Figure 2c is obtained; from this curve, one would estimate that, if the resonator losses are 2% per pass as in Table 1, this FEL should saturate at an intensity of  $\sim 2 \times 10^{10}$  W/cm<sup>2</sup>. Although the curves of Figure 2 are calculated by neglecting all short pulse effects, they should be a good guide to the actual short pulse behavior because, for the system specified by the parameter values of Table 1, the electron pulse length is much longer than the slippage distance. The slippage distance  $s$ , Eq. (12) in Table 2, is the distance that electrons slip behind a light wavefront during one transit of the wiggler because the axial velocity of the electrons is less than the velocity of light. The system studied here has an electron pulse that is 23.7 ns long, as contrasted with the Stanford FEL in which the electron pulse is  $\sim 1.7$  ns.<sup>7</sup> In the latter case, one would not expect cw gain curves to accurately represent the short pulse behavior because a point on the envelope of the electric field would slip approximately one-half the entire electron pulse and thus would be driven by a wide range of different electron densities during one transit through the wiggler.

The gain curves of Figure 2 were calculated assuming coherent light interacting with the electrons in the wiggler. In fact, the initial light in the resonator is incoherent spontaneous emission. We have modeled the development of coherence by starting with thermal light that is described by a Gaussian probability distribution for the real and imaginary components of the electric field:<sup>8</sup>

$$P(E_R, E_I) dE_R dE_I = \frac{1}{\pi E_0^2} \exp \left[ - \left( \frac{E_R^2 + E_I^2}{E_0^2} \right) \right] dE_R dE_I \quad (13)$$

Note that  $\langle E_R \rangle = \langle E_I \rangle = 0$  but  $\langle E_R^2 + E_I^2 \rangle = E_0^2$ , where the average light intensity is given by  $\langle I \rangle = cE_0^2/4\pi$ ;  $\langle I \rangle$  has been chosen to be about that expected for the spontaneous emission intensity for our FEL parameters.<sup>9</sup> Having chosen a particular realization of such an incoherent pulse, the light is propagated through the resonator many times without adding a new incoherent component on each pass as would occur in the actual spontaneous emission process. The results of such a calculation are shown in Figure 3: the initial and final (after 100 passes) intensity profiles are in Figures 3a and 3b; the initial and final spectra are in Figures 3c and 3d (note that the initial spectrum is white noise and does not have the precise form expected of our tapered wiggler); the energy gain vs pass number is in Figure 3e. After 100 passes, the pulse clearly has developed substantial coherence and is growing at a rate consistent with the small signal gain (minus the cavity loss) of Figure 2.

Although this calculation is hardly a precise modeling of the start up of an FEL oscillator from noise, it does indicate that the system specified by Table 1 might start by itself (without injecting an optical pulse generated by another laser source), and it suggests that one needs to add 100 passes to the results to be given in the next section to account for such a build-up. We note here that the calculated amplitude of the pulse after 100 passes, of course, depends upon the cavity loss assumed but also has substantial (factor of 3) fluctuations for different realizations of the initial incoherent light.

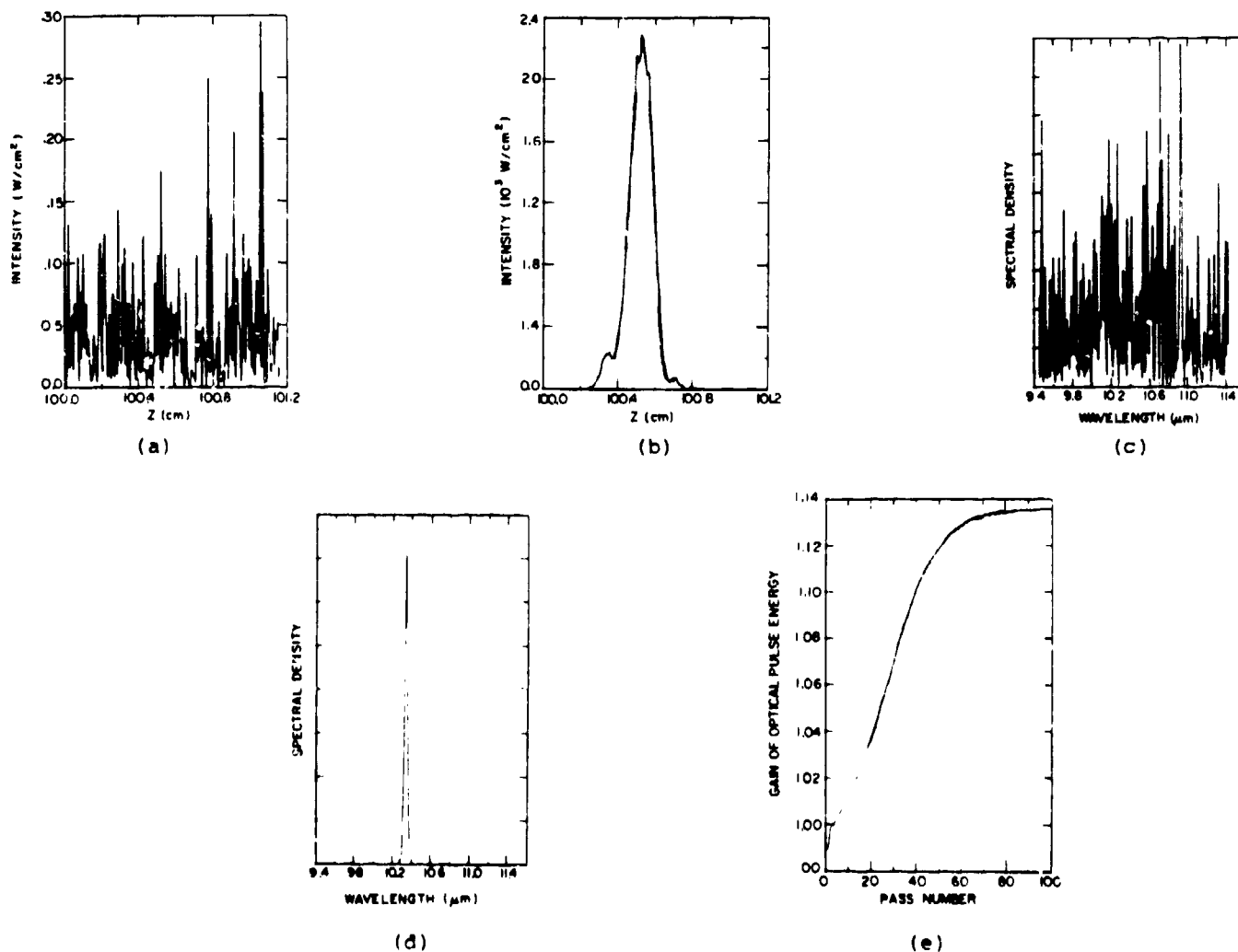


Figure 3. Development of coherence: (a) initial intensity profile; (b) intensity profile after 100 passes; (c) initial spectrum; (d) spectrum after 100 passes; (e) energy gain vs pass number.

#### Transient pulse evolution to quasi steady state

The basic theoretical characteristics of pulse evolution in tapered and untapered wiggler FEL oscillators have been explored in several publications.<sup>3-5, 10-14</sup> Here we present results for the system specified in Table 1, which differ from other work primarily in the ratio (23.7) of the length of the electron pulse to the slippage distance  $s$ . The growth of the the optical pulse energy, and the value of the quasi steady-state energy reached, depend very sensitively upon the deviation of the optical resonator's length from that at exact synchronism: if electron pulses from the linac are injected into the cavity every  $T$  seconds, then the cavity length,  $L_0$ , must be adjusted so that the round-trip time of light,  $2L_0/c$ , equals  $T$ . If this synchronism condition is not met, the light pulse will not overlap the electron pulses (gain media) in the wiggler and thus will decay to zero at a rate determined by the cavity losses. However, the optical pulse shape is distorted by the gain process (laser lethargy) so that the effective pulse velocity is less than  $c$ ; hence the cavity must be shortened slightly to maintain the overlap on successive passes.

Figure 4 shows the growth of the optical pulse energy vs pass number for several resonator lengths different from those at exact synchronism. Figure 5 shows the optical pulse energy after 1900 passes. This curve is not necessarily what one would find after  $10^4$  passes; it is representative of a linac that has a finite macropulse length. In particular, the points at positive values of cavity length change represent pulses that still have finite energy but are decaying away rapidly. One expects this FEL to have an appreciable output only if the resonator length is fixed within range of  $25 \mu\text{m}$  of that at exact synchronism.

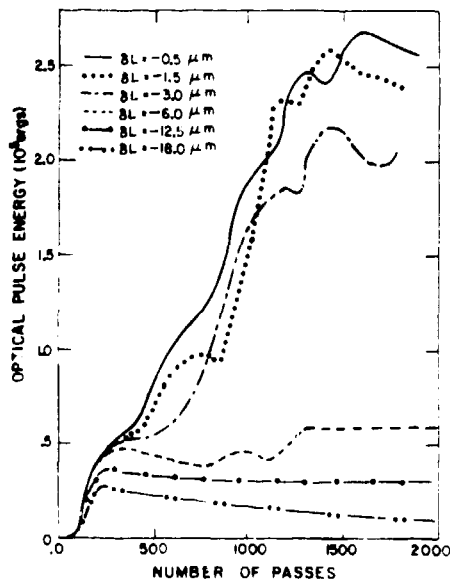


Figure 4. Optical pulse energy vs pass number.

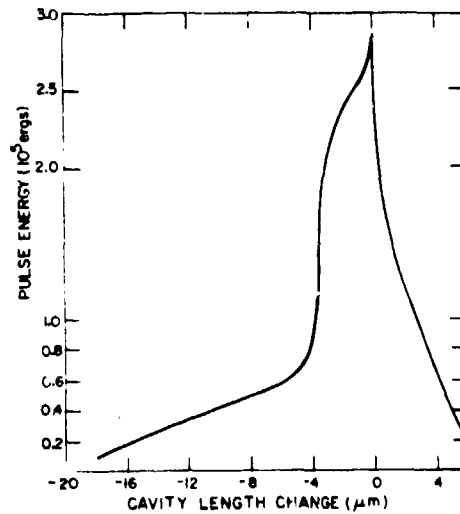


Figure 5. Desynchronization curve.

Figure 6 compares some quasi steady-state optical and electron pulse characteristics for two different cavity length detunings. Figures 6a and 6b show the light intensity vs axial location  $z$  at the end of the wiggler for resonator length detuning of  $-18 \mu\text{m}$  and  $-0.5 \mu\text{m}$ , respectively. Figures 6c and 6d show the optical spectra of these pulses, and Figures 6e and 6f show the corresponding electron spectra (the initial electron beam is monoenergetic with  $\gamma_0 = 40.7932$ ). Figure 6f corresponds to a 2.5% energy-extraction efficiency from the electron beam and exhibits the double-peaked spectrum characteristic of a tapered wiggler.

As is evident from Figure 2, the location of maximum single-pass gain shifts to longer wavelengths with increasing light intensity. Hence, the optical pulse also changes its spectrum (chirps) as the light intensity builds up. The principle mechanism for chirping appears to be the generation of sidebands due to the electrons' synchrotron motion. This in turn implies that the shift in the optical spectrum to longer wavelengths is not continuous with increasing light intensity, but rather occurs in discontinuous steps. Figure 7 illustrates such a step for the  $-0.5\text{-}\mu\text{m}$ -cavity-length detuning case. The evolution of the spectrum after 925 passes to the final shape--which is shown in Figure 6d--is more complicated and less clearly a stepwise process.

The generation of sidebands at high light intensity occurs because the electrons execute synchrotron oscillations,<sup>15</sup> characterized by a period  $L_{sy}$ , in the ponderomotive potential wells.  $L_{sy}$  depends on the light intensity and is given by

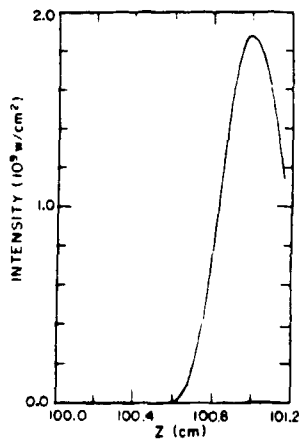
$$L_{sy} = \lambda_w \left( \frac{1 + 0.5 a_w^2}{2Ga_w a_s} \right)^{1/2} \quad (14)$$

This means that the periodicity of the electrons' orbits is given not by the wiggler wave vector  $K_w$  but by  $K_w \pm K_{sy}$ , where  $K_{sy} = 2\pi/L_{sy}$ . Hence, one might expect that this motion would couple to a shifted optical wavelength  $\lambda_B'$  through a modified resonance condition:

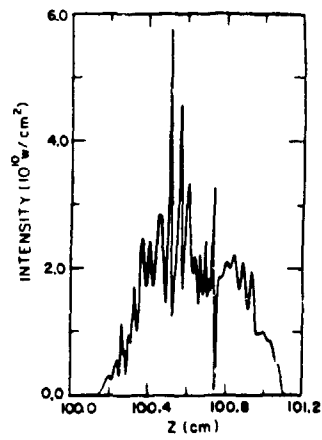
$$K_w \pm K_{sy} = \left( \frac{1 + 0.5 a_w^2}{2\gamma^2} \right) K_B' \quad (15)$$

or

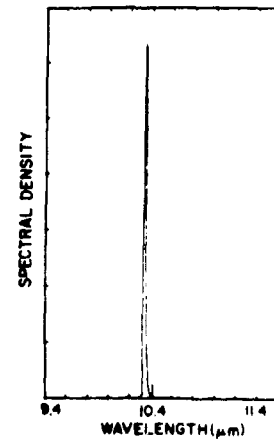
$$\lambda_B' = 2\pi K_B' = \lambda_B \left( 1 \pm \lambda_w / L_{sy} \right) \quad (16)$$



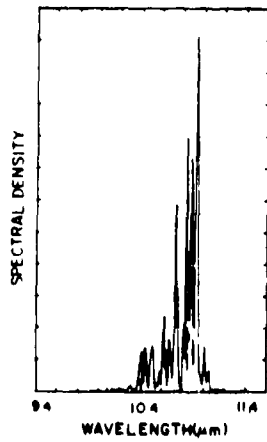
(a)



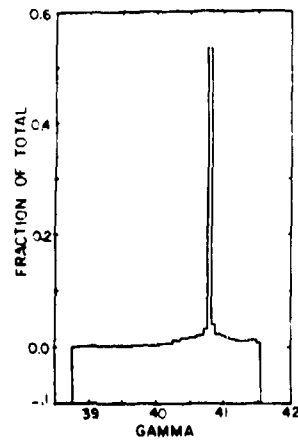
(b)



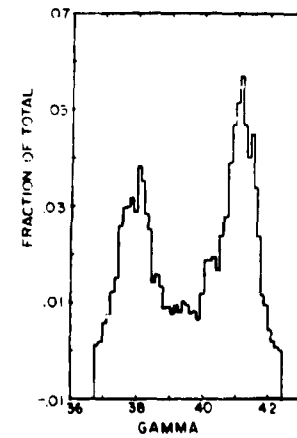
(c)



(d)



(e)

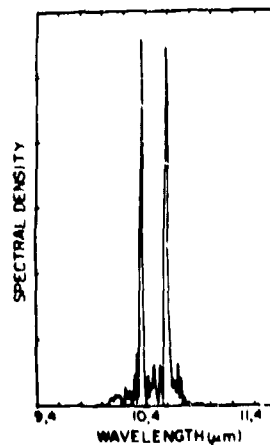


(f)

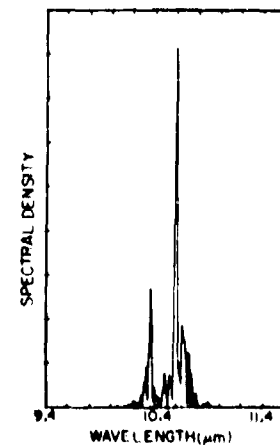
Figure 6. Quasi steady-state pulse characteristics: (a) intensity profile for -18- $\mu\text{m}$  detuning; (b) intensity profile for -0.5- $\mu\text{m}$  detuning; (c) optical spectrum for -18- $\mu\text{m}$  detuning; (d) optical spectrum for -0.5- $\mu\text{m}$  detuning; (e) electron spectrum for -18- $\mu\text{m}$  detuning; (f) electron spectrum for 0.5- $\mu\text{m}$  detuning.



(a)



(b)



(c)

Figure 7. Chirping of optical spectrum by sideband generation: (a) 775 passes; (b) 850 passes; (c) 925 passes.

The presence of a new wavelength  $\lambda_s'$  in the optical spectrum is accompanied by a modulation of the electric-field envelope at a wavelength  $\bar{\lambda}$ :

$$E_{TOT} = E_s \exp(iK_s Z) + E_{s'} \exp(iK_{s'} Z) = E_s \left[ 1 + \frac{E_{s'}}{E_s} \exp(-i\bar{K}Z) \right] \exp(iK_s Z) \quad (17)$$

$$\bar{\lambda} = 2\pi/\bar{K} = \frac{2\pi}{K_s - K_{s'}} = \lambda_s \left( \frac{L_{sy}}{\lambda_w} \right) \quad (18)$$

Because  $L_{sy}$  is a continuous function of the light intensity, provided that the intensity is above the threshold for the definition of the closed-orbit phase-space region ("bucket"), one might expect a continuous generation<sup>15</sup> of sidebands. In calculations with a finite pulse,<sup>5, 10-14</sup> it is found that the envelope of the optical field becomes strongly modulated with  $\bar{\lambda} = s$ , the slippage distance. Recall that  $s$  is the distance over which electrons communicate with each other through the electromagnetic field in one pass through the wiggler. From Eq. (18) this implies that the modulation occurs at an intensity for which  $L_{sy} = L_w$ , the wiggler length. The shift of the sideband in Figure 7 is  $\sim 2.57\%$  from the initial wavelength of 10.35  $\mu\text{m}$ ; this is consistent with the synchrotron period equaling the wiggler length so that  $\lambda_w(1/2)/L_{sy} = \lambda_w(1/2)/L_w = (38.9)^{-1}$ .

#### Operation with an optical filter

The growth of sidebands, and the accompanying modulation of the optical pulse, may not be a desirable effect. Besides broadening the optical spectrum, electron detrapping may occur,<sup>15</sup> thus reducing the extraction efficiency from the electron beam. One way<sup>15, 13</sup> to avoid the effect is to introduce an optical filter into the resonator that attenuates light at the expected sideband wavelength while allowing light at the initial wavelength (peak of the small signal gain) to pass through unattenuated. From Figures 7 and 6d, the optical spectrum in our FEL shifts from 10.35  $\mu\text{m}$  to  $\sim 10.9 \mu\text{m}$ .

We have repeated the calculation of the evolution of the pulse with a -0.5- $\mu\text{m}$  cavity detuning, including an idealized intracavity high-pass optical filter that the light transmits on each pass. The filter transmits, unattenuated, all spectral components with a wavelength less than 10.5  $\mu\text{m}$  and totally deletes all components with a longer wavelength. We neglect any wavelength-dependent phase shift that might accompany such an attenuation pattern.

The results of the calculation are shown in Figure 8. The optical pulse intensity profile and spectrum, after 800 passes, are shown in Figures 8a and 8b. Note that this single-sided filter does not prevent significant upper sidebands from growing. Figures 8c and 8d show the quasi steady-state pulse shape and spectrum after 1600 passes. Although there is short-wavelength structure in the spectrum, its amplitude is only  $\sim 1\%$  or less of the peak. The spectrum is very narrow, apparently largely due to a very linear phase function for the electric field. The accompanying electron spectrum is shown in Figure 8e; the extraction efficiency is  $\sim 2.5\%$ , slightly less than the unfiltered pulse of Figure 6. Hence, it appears that optical filters within the resonator may have substantial beneficial effects, although perhaps not as striking as in this case of a very idealized filter.

#### Conclusions

A tapered wiggler FEL oscillator has been studied within the limitations of a 1-D theoretical model with a realistic set of magnet, electron beam, and optical resonator values. The cw gain curves were calculated at low and high light intensity. A low-amplitude incoherent pulse was shown to develop coherence in 100 passes and subsequently to grow at the expected small signal gain rate. The growth of a coherent pulse from low amplitude to saturation was calculated for various cavity length detunings. High intensity pulses were observed to reach a quasi steady-state within 2000 passes through the resonator. The width of the corresponding desynchronization curve was  $\sim 25 \mu\text{m}$ . A maximum energy-extraction efficiency from the electron beam of 2.8% was observed. The process by which the light adjusted its frequency to follow the change of the gain maximum with increasing light intensity was observed to occur approximately by discrete steps involving the generation of sidebands with frequency steps related to the electron synchrotron frequency. An ideal high-pass optical filter placed in the resonator yielded a very narrow pulse spectrum with little loss in extraction efficiency.

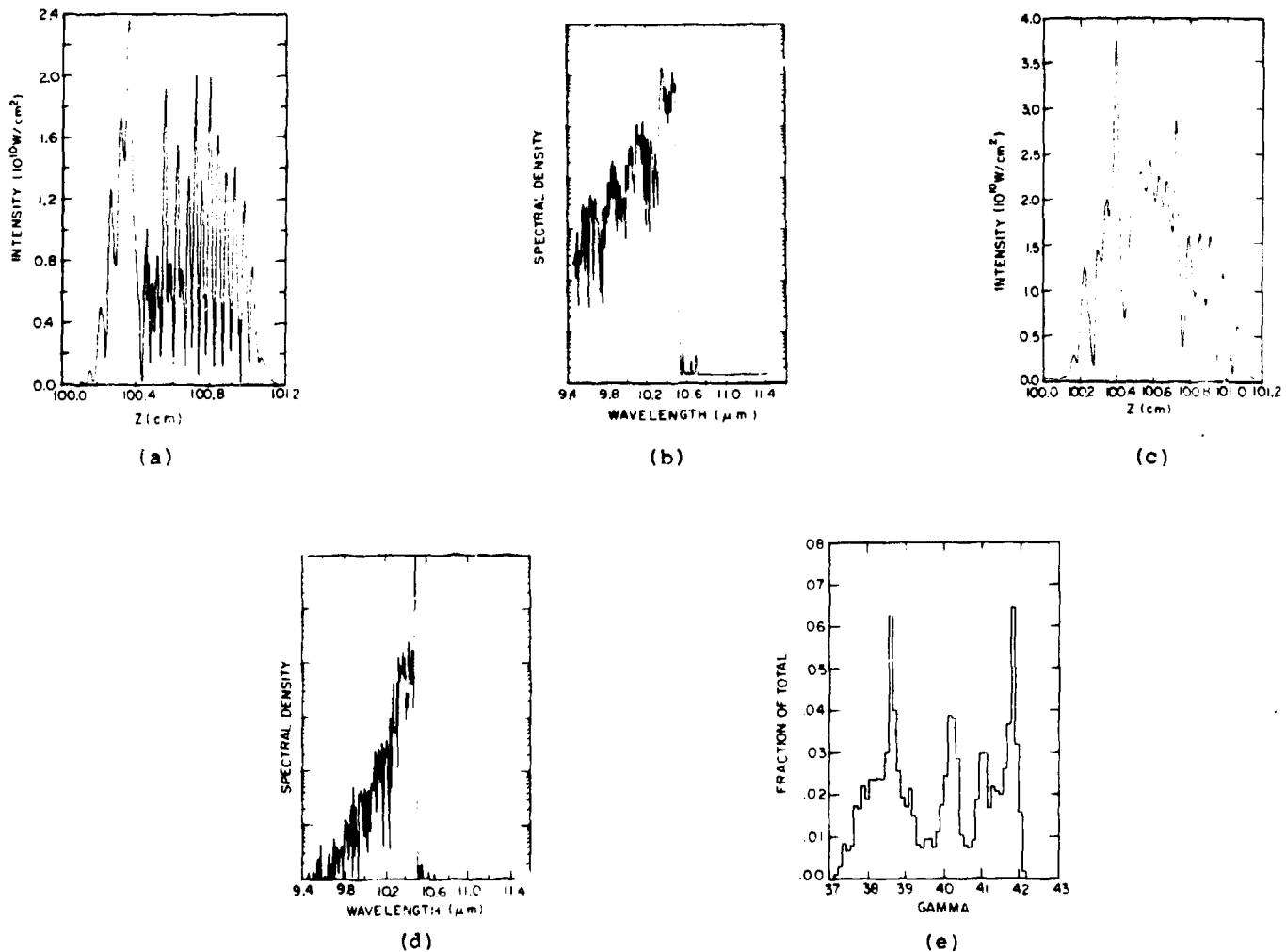


Figure 8. Pulse evolution with an optical filter: (a) intensity profile after 800 passes; (b) spectrum after 800 passes; (c) intensity profile after 1600 passes; (d) spectrum after 1600 passes; (e) electron spectrum after 1600 passes.

#### Acknowledgment

Work performed for the Defense Advanced Research Projects Agency under the auspices of the United States Department of Energy.

#### References

1. Colson, W. B., and Ride, S. K., "The Free-Electron Laser: Maxwell's Equations Driven by Single-Particle Currents," Free-Electron Generators of Coherent Radiation, Physics of Quantum Electronics, Vol. 7, S. F. Jacobs, H. S. Pilloff, M. Sargent III, M. O. Scully, and R. Spitzer, eds. (Addison-Wesley, 1980), p. 377.
2. Colson, W. B., "The Nonlinear Wave Equation for Higher Harmonics in Free-Electron Lasers," IEEE J. Quant. Electron. EQ-17, p. 1417 (August 1981).
3. Al-Abawi, H., McIver, J. K., Moore, G. T., and Scully, M. O., "Pulse Propagation in the Tapered Wiggler," Free Electron Generators of Coherent Radiation, Physics of Quantum Electronics, Vol. 8, S. F. Jacobs, G. T. Moore, H. S. Pilloff, M. Sargent III, M. O. Scully, and R. Spitzer, eds. (Addison-Wesley, 1982), p. 457.
4. Dattoli, G., Marino, A., Renieri, A., and Romanelli, F., "Progress in the Hamiltonian Picture of the Free-Electron Laser," IEEE J. Quant. Electron. QE-17, p. 1371 (August, 1981).

5. Colson, W. B., and Renieri, A., "Pulse Propagation in Free Electron Lasers," Bendor Free Electron Laser Conference, D. A. G. Deacon and M. Billardon eds., Journal de Physique 44, Colloque C1, Supplement 2, p. C1-11 (February 1983).
6. Eckstein, J. N., Madey, J. M. J., Robinson, K., Smith, T. I., Benson, S., Deacon, D., and Taber, R., "Additional Experimental Results from the Stanford 3 Micron FEL," Free Electron Generators of Coherent Radiation, Physics of Quantum Electronics Vol. 8, S. F. Jacobs, G. T. Moore, H. S. Pilloff, M. Sargent III, M. O. Scully, and R. Spitzer eds. (Addison-Wesley, 1982), p. 49.
7. Benson, S., Deacon, D. A. G., Eckstein, J. N., Madey, J. M. J., Robinson, K., Smith, T. I., and Taber, R., "Review of Recent Experimental Results from the Stanford 3- $\mu$ m Free Electron Laser," Bendor Free Electron Laser Conference, David A. G. Deacon and Michel Billardon eds., Journal de Physique 44 Colloque C1, Supplement 2, p. C1-353 (February, 1983).
8. Glauber, R. J., "Optical Coherence and Photon Statistics", in Quantum Optics and Electronics (1964 Les Houches Summer School), C. DeWitt, A. Blandin, and C. Cohen-Tannoudji eds. (Gordon and Breach, 1964), p. 63.
9. Bosco, P., Colson, W. B., and Freedman, R. A., "Quantum/Classical Mode Evolution in Free Electron Laser Oscillators," IEEE J. Quant. Electron. QE-19, p. 272 (March, 1983).
10. Colson, W. B., "Optical Pulse Evolution in the Stanford Free-Electron Laser and in a Tapered Wiggler," Free Electron Generators of Coherent Radiation, Physics of Quantum Electronics Vol. 8, S. F. Jacobs, G. T. Moore, H. S. Pilloff, M. Sargent III, M. O. Scully, and R. Spitzer eds. (Addison-Wesley, 1982), p. 457.
11. Goldstein, J. C., and Colson, W. B., "Pulse Propagation in Free Electron Lasers with a Tapered Undulator," Proceedings of the International Conference on Lasers '81, C. B. Collins, ed. (STS Press, 1982), p. 93.
12. Goldstein, J. C., Colson, W. B., and Warren, R. W., "Tapered Wiggler Free Electron Lasers Driven by Nonmonoenergetic Electron Beams," Bendor Free Electron Laser Conference, D. A. G. Deacon, and M. Billardon eds., Journal de Physique 44, Colloque C1, Supplement 2, p. C1-371 (February, 1983).
13. Goldstein, J. C., and Colson, W. B., "Control of Optical Pulse Modulation due to the Sideband Instability in Free Electron Lasers," Proceedings of the International Conference on Lasers '82, (STS Press), to be published.
14. Goldstein, J. C., "Evolution of Long Pulses in a Tapered Wiggler Free Electron Laser," Proc. 1983 Los Alamos Conference on Optics, SPIE, to be published.
15. Kroll, N. M., and Rosenbluth, M. N., "Sideband Instabilities in Trapped-Particle Free Electron Lasers," Free Electron Generators of Coherent Radiation, Physics of Quantum Electronics Vol. 7, S. F. Jacobs, H. S. Pilloff, M. Sargent III, M. O. Scully, and R. Spitzer eds. (Addison-Wesley, 1980), p. 147.